PCCP

Determination of the structures of benzotriazole$(H_2O)_{1,2}$ clusters by IR–UV spectroscopy and *ab initio* theory

M. Schmitt,* Ch. Plützer and K. Kleinermanns

Heinrich-Heine-Universität Düsseldorf, Universitätsstraße 26.43.02, 40225 Düsseldorf, Germany. E-mail: mschmitt@uni-duesseldorf.de

Received 4th June 2001, Accepted 1st August 2001
First published as an Advance Article on the web 3rd September 2001

The structures of benzotriazole monomer and benzotriazole$(H_2O)_{1,2}$ clusters have been examined by comparison of R2PI spectra and IR–UV double resonance spectra with the results of *ab initio* based normal mode calculations. The structures of the binary benzotriazole–water cluster and the $n = 2$ cluster are shown to be cyclic. Based on these cyclic structures the intermolecular vibronic transitions have been assigned by comparison with *ab initio* normal mode analysis. The cyclic benzotriazole$(H_2O)_{1,2}$ clusters can be viewed as a precursor to a transition state for H-atom transfer from the 1- to the 2-position in benzotriazole. The activation energy for this tautomerism has been calculated for the monomer and the $n = 1$ and 2 cluster as the difference between the stabilization energy of the more stable tautomer and the respective transition state. It has been found to decrease rapidly, with increasing cluster size.

I. Introduction

Benzotriazole can form two different tautomers, the 1*H*- and the 2*H*-benzotriazole, which are shown in Fig. 1. In the hydrogen bonded clusters with water, the water molecule(s) can in principle attach at different positions to the chromophore. Furthermore, due to the close vicinity of proton-donating and proton-accepting groups in benzotriazole, already small water clusters might form cyclic structures. These cyclic cluster structures might assist the tautomerism of 1*H*- and 2*H*-benzotriazole. In order to study this interesting phenomenon, one has to elucidate the structures of the species concerned in the reaction. Benzotriazole contains proton-donating and proton-accepting functional groups, as well as an aromatic π-system. All three regions are potential sites for the binding of one or more water molecules, which may bridge the functional groups. Thus, determination of the equilibrium structure of the benzotriazole–water clusters is a demanding task.

The minimum energy structure of the monomer is not indubitable, due to an equilibrium between different tautomeric forms, which differ in the position of one H-atom and exhibit nearly equal energies. The 1*H*- and 3*H*-tautomers are identical, while the 2*H*-tautomer differs in energy. For the benzotriazole monomer we could show experimentally, that the most stable form is the 1*H*-tautomer (equal to the 3*H*-tautomer).[1] The energy difference between the 1*H*- and the 2*H*-tautomer has been determined by recording the FTIR spectra of both tautomers at different temperatures to be 417 cm^{-1}.[1] This small energy difference explains the great expenditure both in theoretical methods and in basis sets, which has to be pursued in determining the most stable structures.

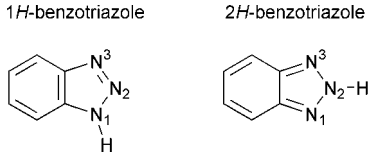

Fig. 1 The two tautomeric forms of benzotriazole and the atomic numbering which is used in the text.

Benzotriazole has been studied both experimentally and theoretically. The microwave spectra of 1*H*-benzotriazole have been measured both in a gas cell[2] and in a molecular beam.[3] The vibrationless $S_1 \leftarrow S_0$ transition of benzotriazole at 34 920 cm^{-1}, which was observed first by Jalviste *et al.*[4] was shown to be due to the 2*H*-tautomer using rotationally resolved LIF spectroscopy.[5] The dispersed fluorescence spectra of benzotriazole taken in our group could be assigned to be solely due to 2*H*-benzotriazole.[6] Fourier transform infrared spectra of benzotriazole in a molecular beam in the range 650–1700 cm^{-1} showed vibrational bands, which could be attributed to 2*H*-benzotriazole,[7] while infrared spectra in the solid state were assigned as belonging to 1*H*-benzotriazole.[7,8]

From a comparison of the UV band spectra of benzotriazole with the spectra of the 1- and 2-methyl-substituted derivatives at different temperatures Catalán *et al.* concluded, that up to 20% of 2H-BT are present in the gas phase at 90 °C.[9,10] While Hartree–Fock calculations predict the 1*H*-tautomer to be favored by ≈800–1000 cm^{-1}, this ordering is reversed when electron correlation effects are included *via* second-order Møller-Plesset perturbation theory.[10]

Recently we presented an analysis of the S_1 spectrum of the binary benzotriazole–water cluster and a comparison with the binary benzimidazole–water cluster.[11] Here we analyze the intramolecular –OH and –NH stretching vibrations in the electronic ground state of benzotriazole$(H_2O)_{0,1,2}$, in order to determine the structure of the benzotriazole–water clusters by comparison with the results of an *ab initio* based normal mode analysis.

II. Experimental set-up

The experimental set-up for the resonance enhanced two-photon ionization (R2PI) and UV–UV spectral hole burning (SHB) is described in detail elsewhere.[6,12] Briefly, the apparatus consists of a source chamber pumped with a 1000 l s^{-1} oil diffusion pump (Alcatel) in which the molecular beam is formed by expanding a mixture of helium and benzotriazole through the 300 μm orifice of a pulsed nozzle (General Valve, Iota One). Dried benzotriazole was heated to 100 °C prior to

 DOI: 10.1039/b104889a

expansion in He. The spectra of the deuterated substances were recorded by simply flowing D_2O vapor at a partial pressure of 18 mbar over the solid benzotriazole sample and recording successively the R2PI spectra. The water clusters were formed by co-expanding water at a partial pressure of 10 mbar. The skimmed molecular beam (Beam Dynamics Skimmer, 1 mm orifice) crosses the laser beams at right angles in the ionization chamber. The ions are extracted in a gridless Wiley–McLaren type time-of-flight (TOF) spectrometer (Bergmann Meßgeräte Entwicklung) perpendicular to the molecular beam and laser direction and enter the third (drift) chamber where they are detected using multi-channel plates (Galileo). Ionization and drift chamber are both pumped with a 150 l s^{-1} rotatory pump (Leybold). The vacuum in the three chambers with molecular beam on was 1×10^{-3} mbar (source), 5×10^{-5} mbar (ionization) and 1×10^{-7} mbar (drift), respectively. The resulting TOF signal was digitized by a 500 MHz oscilloscope (TDS 520A, Tektronix) and transferred to a personal computer, where the TOF spectrum was recorded and stored.

The R2PI measurements were carried out using the frequency doubled output of a Nd : YAG (Spectra Physics, GCR170) pumped dye laser (LAS, LDL205) operated with Fluorescein 27. For UV–UV hole burning spectroscopy the second harmonic of a Nd : YAG (Spectra Physics GCR3) pumped dye laser (LAS, LDL205) operated with Fluorescein 27 dye was used. Both lasers have been calibrated by comparison with the tabulated transition frequencies to the iodine spectrum.

For IR–UV hole burning we used an infrared dye (a mixture of Styryl 8 and Styryl 9) whose radiation is aligned collinear with the perpendicularly polarized Nd-YAG fundamental (1064 nm) and directed through a MgO-doped $LiNbO_3$ crystal to generate 3200–4000 cm^{-1} radiation *via* difference frequency mixing. Suitable dielectric mirrors separate the Nd-YAG fundamental and the dye laser beam behind the $LiNbO_3$ crystal. We typically use 50 mJ $(pulse)^{-1}$ of the YAG fundamental and 15–20 mJ $(pulse)^{-1}$ of the dye laser output to obtain 1–3 mJ $(pulse)^{-1}$ IR radiation between 3200 and 4000 cm^{-1} with a bandwidth of <0.1 cm^{-1}. The IR laser was calibrated by recording a water vapor spectrum and comparing the lines to a literature spectrum.[13]

The UV–IR spectra have been taken at a fixed IR wavelength, with the UV-laser scanned over the region of interest. The resulting spectrum is obtained by subtracting the UV–IR-double resonance spectrum from the R2PI spectrum, after normalizing them to the same peak area. The experiment control software was modified in order to record the R2PI spectrum (UV) and the UV–IR spectra at each spectral position simultaneously. This is necessary to minimize the errors due to changing conditions during the scans.

III. Theoretical methods

All *ab initio* calculations were performed using the GAUSSIAN 98 program package.[14] The SCF energy convergence criterion used was 10^{-8} E_h and the convergence criterion for the gradient optimization of the molecular geometries of the cluster structures was 1.5×10^{-5} E_h a_0^{-1} and $E_h(\text{degree})^{-1}$, respectively. However, for the benzotriazole$(H_2O)_2$ clusters more relaxed convergency criteria of 10^{-5} E_h for the SCF energy and 4.5×10^{-4} E_h a_0^{-1} and $E_h(\text{degree})^{-1}$, respectively had to be employed, in order to keep the computing time within reasonable limits.

The geometry optimization of the different benzotriazole clusters was performed using Møller–Plesset perturbation theory at second-order (MP2) level using the 6-31G(d,p) basis set. The vibrational frequencies of the electronic ground state were calculated using the analytical second derivatives of the MP2 potential energy surface. The intermolecular frequencies for the electronically excited state of the benzotriazole–water clusters were calculated using the configuration interaction method with single excitations (CIS).

The stabilization energies D_e and D_0 for the clusters were obtained as differences of the cluster and monomer energies and are corrected for the zero-point energy (ZPE) and the basis set superposition error (BSSE) using the counterpoise method of Boys and Bernardi.[15]

The transition states (TS) for the tautomerization equilibria have been optimized using the synchronous transit-guided quasi-Newton (STQN) Method of Schlegel and coworkers[16,17] using the corresponding optimized cluster structures at the minima of the potential which are connected by the TS.

IV. Results

A. The benzotriazole monomer

Using FTIR spectroscopy, the frequency of the N–H stretching vibration of 2*H*-benzotriazole was determined experimentally to be 3489 cm^{-1}, while the 1*H*-tautomer has a slightly higher vibrational frequency of 3511 cm^{-1} in the gas phase.[1] Berden *et al.*[5] showed that the electronic origin of benzotriazole at 34 917.8 cm^{-1} belongs to the 2*H*-tautomer.

The frequency of the N–H stretching vibration of 2*H*-benzotriazole was calculated to 3696.6 cm^{-1} at the MP2/6-31G(d,p) level, while the corresponding frequency of 1*H*-benzotriazole was determined to be 3724.1 cm^{-1} using the same method and basis set.

1. IR–UV hole burning. The electronic origin cannot be observed under one-color conditions, because the S_1–D_0 distance is larger than S_0–S_1. Therefore we measured the IR–UV double resonance spectrum of the benzotriazole monomer upon analysis of the vibronic band at 35 400.8 cm^{-1}, which is a very intense vibronic band in the R2PI spectrum of the monomer (*cf.* Table 1). The spectrum, Fig. 2a, shows only one peak at 3488.4 cm^{-1}. This value matches the FTIR frequency of the N–H stretching vibration of 2*H*-benzotriazole very well, which proves the above assumption that the electronic origin at 34 917.8 cm^{-1} belongs to the 2*H*-tautomer. In order to search for the hitherto unknown electronic origin of 1*H*-benzotriazole we set the IR-laser to the N–H stretching vibration of this tautomer at 3510.4 cm^{-1} and scanned the UV-laser between 35 380 and 35 535 cm^{-1} and between 35 700 and 36 000 cm^{-1}. No difference was detected without the IR-

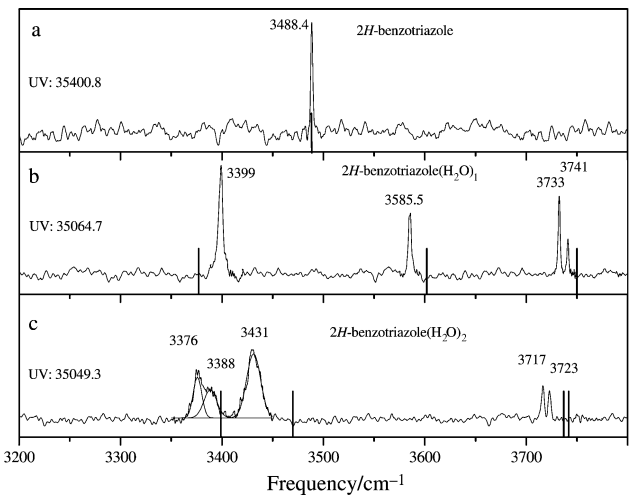

Fig. 2 IR–UV double resonance spectra of (a) 2*H*-benzotriazole; (b) 2*H*-benzotriazole$(H_2O)_1$; (c) 2*H*-benzotriazole$(H_2O)_2$ obtained *via* analysis of the electronic origins given in Table 1. The calculated frequencies (see text) scaled to the frequency of the –NH stretch vibration of the monomer are shown as vertical bars.

Table 1 Electronic origins and spectral shifts of the benzotriazole–water clusters and some of their isotopomers relative to the origin of the 2*H*-benzotriazole monomer

Isotopomer[a]	Electronic origin/cm^{-1}	Spectral shift/cm^{-1}
2*H*-benzotriazole	34 917.8	—
2*D*-benzotriazole	34 971.5	53.7
2*H*-benzotriazole$(H_2O)_1$	35 039.2	121.4
2*D*-benzotriazole$(H_2O)_1$	35 082.2	164.4
2*H*-benzotriazole$(H^bOD^f)_1$	35 039.4	121.6
2*H*-benzotriazole$(D^bOH^f)_1$	35 028.8	111.0
2*H*-benzotriazole$(H_2O)_2$	35 049.3	131.5

[a] The superscripts b and f refer to the hydrogen bound and free H-atom in the cyclic binary cluster.

laser. In contrast to the UV–UV double resonance experiments described in ref. 6 the UV–IR set-up has the advantage, that a transition is utilized, which is known to belong to 1*H*-benzotriazole. Nevertheless in the examined region no absorption due to 1*H*-benzotriazole could be found.

B. The benzotriazole$(H_2O)_1$-cluster

Due to the =N– and >NH functions in the five-membered ring of the 1*H*- and 2*H*-tautomers of benzotriazole, it can act both as proton donor and acceptor in a hydrogen bond with one water molecule. Furthermore, the water moiety could be bound *via* the π-electron cloud of the five- or six-membered ring. However, for these π-bound structures no minima at the potential energy surface could be found. We optimized linear structures with 1*H*- and 2*H*-benzotriazole acting as proton donor towards the water moiety, linear structures in which they act as proton acceptor and cyclic structures in which the >NH function acts as proton donor and =N– as proton acceptor. The MP2/6-31G(d,p) optimized structures are shown in Fig. 3. The corresponding calculated stabilization energies are given in Table 2. The calculations yield linear and >NH···OH···N= cyclic arrangements with similar stabilization energies. The linear structure of 2*H*-benzotriazole-

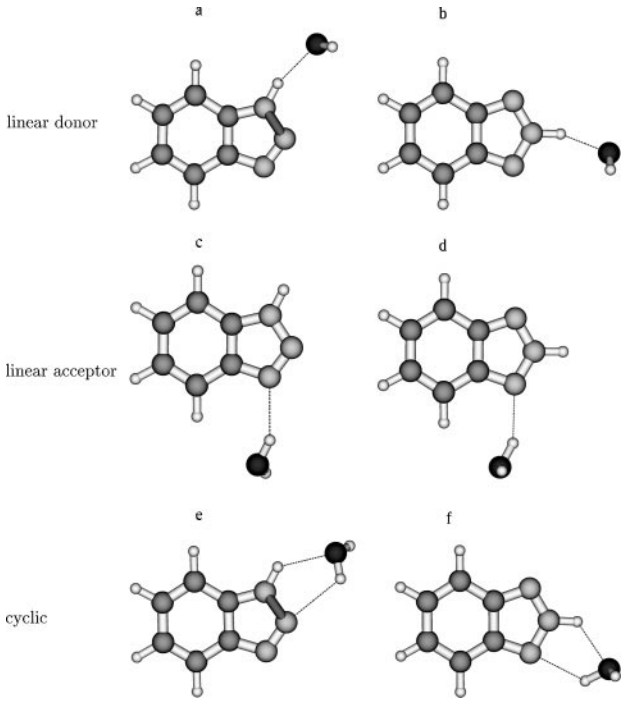

Fig. 3 Optimized structures of six different benzotriazole$(H_2O)_1$ clusters at the MP2/6-31G(d,p) level of theory. The first column shows the 1*H*-benzotriazole clusters, the second column shows the 2*H*-benzotriazole clusters.

Table 2 Absolute and relative stabilization energies of 1*H*- and 2*H*-benzotriazole$(H_2O)_1$ clusters. All calculations have been performed at the MP2 level with the 6-31G(d,p) basis set. Both D_e and D_0 include corrections for the BSSE

Geometry	Structure (Fig. 3)	Energy /E_h	D_e/ kJ mol^{-1}	D_0/ kJ mol^{-1}
Linear, BT donor				
1*H*-BT$(H_2O)_1$	a	−470.948 10	−21.6	−17.6
2*H*-BT$(H_2O)_1$	b[a]	−470.951 26	−29.8	−23.8
Linear, BT acceptor				
1*H*-BT$(H_2O)_1$	c	−470.946 71	−14.0	−8.3
2*H*-BT$(H_2O)_1$	d	−470.948 21	−16.8	−8.8
Cyclic				
1*H*-BT$(H_2O)_1$	e	−470.949 89	−21.7	−15.4
2*H*-BT$(H_2O)_1$	f	−470.952 98	−29.0	−20.4

[a] First-order saddle point.

[donor]$(H_2O)_1$ was found to be a first-order saddle point instead of a true minimum. The zero point energy correction in this case was performed considering only the $3N-7$ normal modes, for which the derivative of the potential energy with respect to the normal coordinates $\partial V/\partial q_i$ equals zero. This structure is a transition state, connecting two cyclic forms of the cluster. The coordinate for this transition is a rotation of the water about its inertial *b*-axis. The fact, that the transition state is energetically below the cyclic minima is an artefact of the BSSE correction on very near structures.

The discussion of the absolute and relative cluster stabilities is complicated by the difficulties arising from the very similar energies of the two *tautomers* as shown in ref. 1. The calculated absolute and relative energies of the clusters, including BSSE and ZPE corrections are given in Table 2. The cyclic and the linear 2*H*-benzotriazole$(H_2O)_1$ cluster in which BT acts as proton donor have the largest stabilization energies D_0 of 20.4 and 23.8 kJ mol^{-1}, respectively. The linear cluster with BT acting as proton acceptor has a considerably lower stabilization energy (8.3 and 8.8 kJ mol^{-1}). In all cases, the 1*H*-cluster was found to be less stable than the 2*H*-cluster.

1. R2PI spectra. Fig. 4 shows the R2PI spectrum of the benzotriazole$(H_2O)_1$ cluster recorded at the mass channel of this cluster. No fragmentation was observed for this, nor for the $n=2$ cluster. The frequency of the electronic origin, which is given in Table 1, is blueshifted with respect to the origin of the monomer by 121.4 cm^{-1}. The UV–UV double resonance spectrum of the benzotriazole$(H_2O)_1$ cluster proves, that all

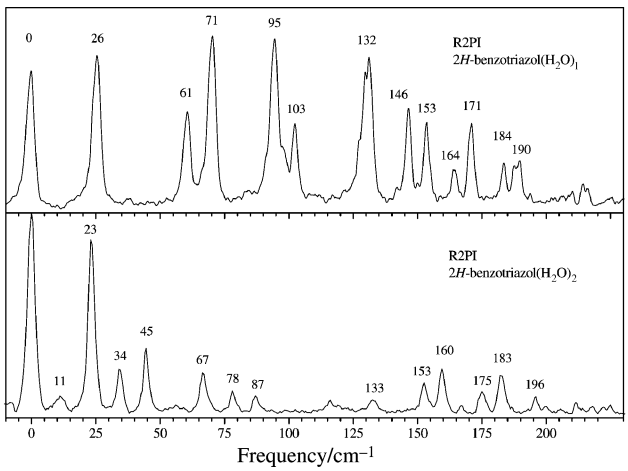

Fig. 4 R2PI spectra of the 2*H*-benzotriazole$(H_2O)_{1,2}$ clusters in the region of the intermolecular vibrations. The frequencies are given relative to the electronic origins at 35 039.2 and 35 049.3 cm^{-1}, respectively.

vibronic transitions in the R2PI spectrum belong to only one conformer of the benzotriazole–water cluster.[11] The relatively small shift to the electronic origin of the 2*H*-tautomer is a strong indication that the water cluster is formed in this tautomeric form too. Within a few thousand wavenumbers no band of the other tautomer could be found.

The complete vibronic spectrum appears also in combination with a prominent vibronic transition at 71 cm^{-1}. A large geometry change upon electronic excitation along this coordinate can be postulated due to the uncommon Franck–Condon pattern. The UV–UV double resonance spectrum proved that both band system origins and all observed bands belong to the same ground state species.[11] Therefore the existence of a tunneling splitting in the electronic ground state which might lead to the observed two nearly identical band systems can be ruled out. Nevertheless a splitting in the S_1-state cannot be ruled out as being responsible for the two band systems.

In order to distinguish between the cyclic and the linear form of the cluster, we performed R2PI spectroscopy on the singly deuterated cluster. For a linear donor cluster one would expect two different electronic origins, namely 2*D*-benzotriazole$(H_2O)_1$ and 2*H*-benzotriazole$(HDO)_1$ with the two positions in the water moiety being equivalent. On the other hand the two positions in the water moiety are distinguishable for the cyclic cluster and therefore should lead to three different electronic origins. Fig. 5 shows the R2PI spectrum recorded on the mass trace of the singly deuterated cluster in the region of the electronic origin. One vibronic progression clearly builds upon an origin (35 039.4 cm^{-1} indicated by b in Fig. 5) which is only slightly shifted with respect to the origin of the undeuterated cluster (35 039.2 cm^{-1}). A second progression can be observed upon an origin, redshifted by 10.6 cm^{-1} with respect to the first origin (a in Fig. 5). A third progression builds upon an origin at 35 082.2 cm^{-1} (c in Fig. 5), thus blueshifted by 42.8 cm^{-1} relative to the origin b. The vibronic patterns built upon all three origins are virtually the same. The blueshift of origin c is similar to the value of the isotopic shift of 53.7 cm^{-1} of 2*H*-benzotriazole/2*D*-benzotriazole.[11] We therefore assign the origin at 35 082.2 cm^{-1} to the isotopomer 2*D*-benzotriazole$(H_2O)_1$. Concerning the assignment of the other two electronic origins we performed an IR–UV double resonance experiment, which will be described in the next section.

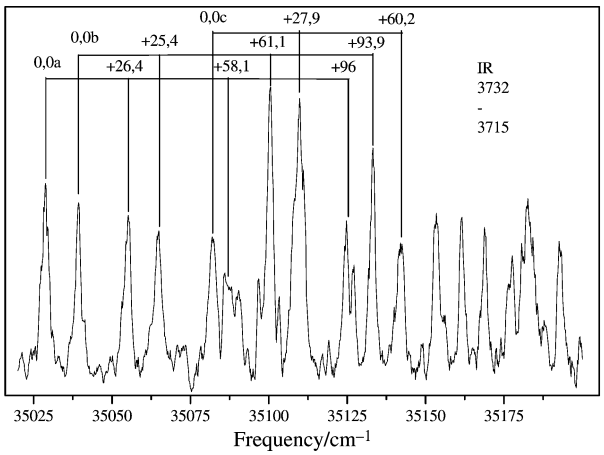

Fig. 5 R2PI-spectrum of the singly deuterated benzotriazole(water)$_1$ cluster in the region of the electronic origin.

2. IR–UV hole burning. Examination of the spectral region of the –NH and –OH stretching vibrations can be helpful in determining the cluster structure, or at least the connectivities of the different cluster moieties. Fig. 2b shows the IR–UV hole burning spectrum of the binary benzotriazole water cluster, obtained upon analysis *via* the band at 35 064.7 cm^{-1} (0.0 + 25.5 cm^{-1}). This band has been chosen, because it is the strongest transition in the R2PI spectrum of the binary cluster. In the region of the –NH and –OH stretching vibrations four bands are observed and compiled in Table 3. The first band at 3399 cm^{-1} can be assigned to a bound –NH stretching vibration. It is redshifted relative to the free –NH vibration by 89.4 cm^{-1} and is broadened compared to the free –NH vibration, which is typical for hydrogen bound –NH stretching vibrations. The observed redshift is the same as reported by Carney *et al.*[18,19] for the related indole–water system. The redshift of the bound –NH vibration proves that benzotriazole acts as a proton donor in this cluster, which causes a weakening of the N–H bond strength. Any of the structures c and d in Fig. 3 in which the water moiety acts as proton donor can therefore be excluded. The next band at 3585.5 cm^{-1} can be assigned to a bound –OH stretching vibration of the water moiety, thus confirming a cyclic structure of the cluster.

The other two bands at 3732.6 and 3740.9 cm^{-1}, respectively, can be assigned to a free –OH stretching vibration of the water moiety, which is split into two components by a large amplitude motion. The existence of two isomers in the ground state, which might be responsible for the occurrence of two different –OH stretching vibrations has already been discarded by UV–UV double resonance spectroscopy.[11] Nevertheless UV–UV hole burning spectroscopy bears the risk of exciting simultaneously two different bands with the probe laser, if they overlap within the bandwidth of the exciting laser. Therefore we analyzed directly through the distinguishable vibrational bands at 3732.6 and 3740.9 cm^{-1} while scanning the UV-laser in the region of interest. Fig. 6 shows the R2PI (a) and UV–IR (b) double resonance spectra obtained by exciting the IR band at 3740.5 cm^{-1}, together with the difference of the normalized spectra (c). Obviously all the bands in the scanned region belong to the analyzed species.

Finally we were able to assign the three electronic origins of the singly deuterated cluster to the corresponding tautomers using IR–UV double resonance. Fig. 7 shows three IR–UV double resonance spectra in the region of the free –OH vibra-

Table 3 Experimental IR frequencies in cm^{-1} of benzotriazole$(H_2O)_1$ in the region of the –NH and –OH stretching vibrations together with calculated vibrational frequencies for different cluster structures. All calculations are performed at the MP2/6-31G(d,p) level of theory. All frequencies have been scaled by 0.95

		1*H*-BT$(H_2O)_1$			2*H*-BT$(H_2O)_1$		
Assignment[a]	Experiment	a[b]	c	e	b	d	f
NH (bound)	3399.0	3315	3534	3407	3304	3511	3399
OH (bound)	3585.5	—	—	3625	—	—	3626
	3732.6	3677	3586	—	3678	3629	—
OH (free)				3779			3775
	3740.9	3800	3777		3802	3781	

[a] The assignment is valid only for the cyclic structures. [b] This designation refers to Fig. 3 and Table 2.

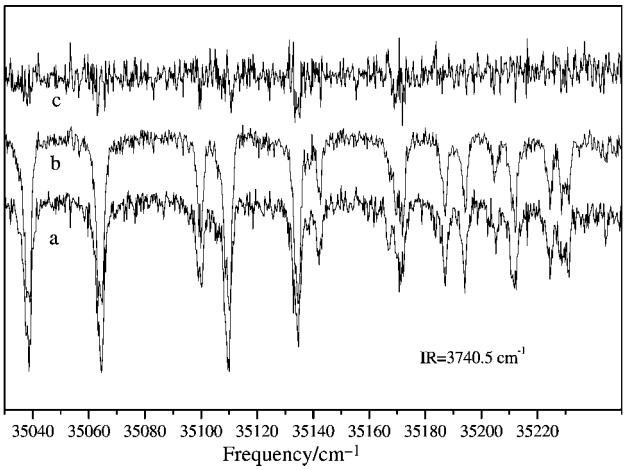

Fig. 6 UV–IR double resonance spectrum of 2*H*-benzotriazole$(H_2O)_1$ obtained with the IR-laser fixed at 3740.5 cm^{-1} (a) and the normalized R2PI spectrum in the same region (b), together with the difference between both spectra (c).

tion, obtained by analyzing the electronic origins of the d_1-isotopomers a, b and c, shown in Fig. 5. All three spectra are different, which proves our assumption of three distinct electronic origins. Analyzing the origin a at 35 039.4 cm^{-1}, we obtained an –OH stretch band at 3715 cm^{-1}. When analyzing the origin c at 35 082.2 cm^{-1} we observed an –OH stretching frequency of 3732 cm^{-1} which is close to the value for the undeuterated cluster. Upon analysis of origin b (35 039.4 cm^{-1}) we did not observe any free –OH stretch band. From this we can deduce that origin b has to be assigned to the 2*H*-benzotriazole$(HOD^f)_1$ cluster in which the deuterium occupies the *free* site, while the origin a at 35 028.8 cm^{-1} is due to 2*H*-benzotriazole$(D^bOH)_1$ in which the deuterium is located at the *bound* site. The free –OH vibration of 2*D*-benzotriazole$(H_2O)_1$ is influenced least of all, so that origin c can safely be assigned to this isotopomer, in coincidence with our findings from R2PI spectroscopy. The assignment of all electronic origins of the isotopmeric clusters is given in Table 1.

3. The benzotriazole$(H_2O)_2$ cluster. In order to determine the structures of the benzotriazole$(H_2O)_2$ cluster several starting geometries, which are shown in Fig. 8, have been considered. Two cyclic structures (one for 1*H*-benzotriazole, the other for 2*H*-benzotriazole) with the two water moieties bridging the functional groups of the five-membered ring (Fig. 8a and b), two linear structures, in which benzotriazole acts as proton acceptor *vs.* a hydrogen bound water dimer (Fig. 8c and d), two linear structures in which the >NH functional group acts as proton donor with respect to one of the water molecule and the =N– group as proton acceptor to the second

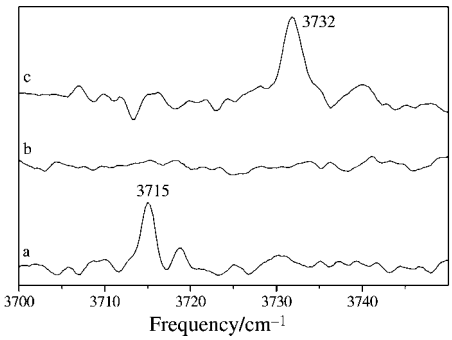

Fig. 7 IR–UV spectra taken by analyzing the three electronic origins of the different d_1-isotopomers, which are shown in Fig. 5.

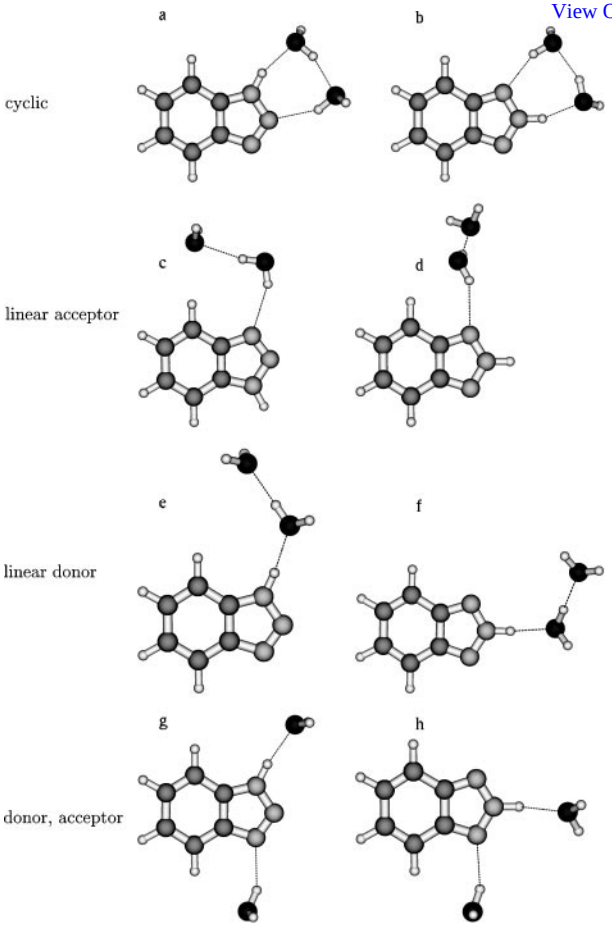

Fig. 8 Eight different starting geometries for the calculation of the benzotriazole$(H_2O)_2$ cluster at the MP2/6-31G(d,p) level of theory.

water molecule (Fig. 8e and f) and two linear structures, in which one water molecule acts as proton donor *vs.* benzotriazole and the other as proton acceptor (Fig. 8g and h).

Starting with these eight geometries, only five converged at the MP2/6-31G(d,p) level of theory to the optimized start geometry. These are the cyclic 1*H*-benzotriazole$(H_2O)_2$ (a) and 2*H*-benzotriazole$(H_2O)_2$ (b) structures, a linear water chain cluster in which BT acts as proton acceptor (c and d) and the linear 1*H*-benzotriazole$(H_2O)_2$ (g) structure in which one water molecule acts as proton donor, the other as proton acceptor. The stationary points at the PES for the linear chain clusters (c and d) turned out to be first order saddle points. Table 4 gives the relative stabilization energies of these five structures. The other starting geometries converged into the cyclic structures a and b. Table 4 summarizes the stabilization energies of these clusters with ZPE correction and BSSE included. The cyclic clusters turn out to be the most stable ones ($D_0 = -59.1$ kJ mol^{-1} for the 2*H*-cluster and -57.2 kJ mol^{-1} for the 1*H*-cluster). The stabilization energy for the linear chain cluster with benzotriazole acting as proton acceptor was calculated to be -29.5 and -19.6 kJ mol^{-1} for the 1*H*- and 2*H*-cluster, respectively. The linear 1*H*-benzotriazole$(H_2O)_2$ structure in which one water molecule acts as proton donor, the other as proton acceptor is stabilized with respect to the monomers by -34.9 kJ mol^{-1}.

4. R2PI spectra. The electronic origin of the $n = 2$ cluster is shifted by 131.5 cm^{-1} to higher energy compared to the monomer (Fig. 4c). This is a shift of only 10 cm^{-1} further to the blue than the origin of the binary cluster, as shown in Table 1. The Franck–Condon pattern in the spectrum of the 2*H*-benzotriazole$(H_2O)_2$ cluster points to similar structures in

Table 4 Absolute and relative stabilization energies of several benzotriazole$(H_2O)_2$ clusters. All calculations have been performed at the MP2 level with the 6-31G(d,p) basis set. Both D_e and D_0 include corrections for the BSSE

Geometry	Structure (Fig. 8)	Energy /E_h	D_e/ kJ mol^{-1}	D_0 kJ mol^{-1}
Cyclic				
1*H*-BT$(H_2O)_2$	a	−547.196 51	−75.6	−57.2
2*H*-BT$(H_2O)_2$	b	−547.197 52	−78.8	−59.1
Linear chain, BT acceptor				
1*H*-BT$(H_2O)_2$	c[a]	−547.179 32	−42.9	−29.5
2*H*-BT$(H_2O)_2$	d[a]	−547.177 99	−34.3	−19.6
Linear chain, BT donor				
1*H*-BT$(H_2O)_2$	e	converges to a	—	—
2*H*-BT$(H_2O)_2$	f	converges to b	—	—
Linear, BT donor and acceptor				
1*H*-BT$(H_2O)_2$	g	−547.183 25	−47.8	−34.9
2*H*-BT$(H_2O)_2$	h	converges to b	—	—

[a] First-order saddle points at the PES. The ZPE corrections have been calculated along the $3N - 7$ normal modes, for which $(\partial V/\partial q_i) = 0$.

electronic ground and excited state, in contrast to the spectrum of 2*H*-benzotriazole$(H_2O)_1$. A comparison of the experimental vibronic frequencies with an *ab initio* based normal mode analysis will be discussed after determination of the structure with IR–UV double resonance spectroscopy in the next section.

5. IR–UV hole burning. The IR–UV hole burning spectrum of benzotriazole$(H_2O)_2$ obtained upon analysis of the electronic origin at 35 049.3 cm^{-1} is shown in Fig. 2c. Here the assignment of the intramolecular vibrations to a certain cluster structure is straightforward. For a cyclic cluster, as shown in Fig. 8a and b, one expects two free –OH vibrations, two bound –OH and one bound –NH stretching vibration. The spectrum in Fig. 2c shows a band at 3376 cm^{-1}, which might be assigned to the NH stretching vibration. It is redshifted by 23 cm^{-1} compared to the binary cluster and by 112 cm^{-1} compared to the free –NH vibration of the monomer. A band analysis of the overlapping bands at 3376 and 3388 cm^{-1} shows that the band which is assigned to the bound –NH stretching vibration is further broadened compared to the binary cluster. However, if one compares the calculated frequency of the bound –NH stretching vibration to the experimental value, it is striking that there is a large discrepancy. While the red shift of the binary cluster to the free –NH vibration of benzotriazole is reproduced quite well (experimental value: 89 cm^{-1}, calculated shift: 146 cm^{-1} for the cyclic cluster), the calculated shift for the 1 : 2 cluster deviates considerably (experimental value: 112 cm^{-1}, calculated shift: 467 cm^{-1} for the cyclic cluster). Therefore it is possible, that the bound –NH stretching vibration is shifted below 3200 cm^{-1}. Unfortunately this range was experimentally not accessible for us. If the band at 3376 cm^{-1} is not the bound –NH vibration, another interpretation has to be given. The explanation that this band is due to a Fermi resonance of one of the bound –OH stretching vibrations with an overtone of the water bending mode, as discussed by Watanabe *et al.*[20] for the cyclic phenol–water clusters is very unlikely, because the highest value found for an water bending mode in a hydrogen bonded cluster is 1640 cm^{-1}, as determined by Paul *et al.*[21] An overtone of this band would not be expected to be further blue shifted by 100 cm^{-1}.

The next two (broad) transitions at 3388 and 3431 cm^{-1} are due to the two bound –OH stretching vibrations. Compared to the phenol$(H_2O)_2$ system in which these two vibrations are observed at 3505 and 3552 cm^{-1}, they are redshifted.[22] The free –OH stretching vibrations are observed at 3717 and 3723 cm^{-1}, in very good agreement with the phenol$(H_2O)_2$ values of 3722 and 3725 cm^{-1}. Comparison of the experimental vibrational frequencies with the calculated frequencies of the cyclic 2*H*-benzotriazole$(H_2O)_2$ cluster gives a good agreement, *cf.* Table 5. Again, from the close agreement of the electronic origin of the benzotriazole monomer with the origin of the $n = 2$ cluster we suppose that the cluster is in the 2*H*-form.

C. Transition states for the tautomerization

1. Benzotriazole. The transition state for the tautomerization reaction between 1*H*-benzotriazole and 2*H*-benzotriazole has been calculated at the MP2/6-31G(d,p) level of theory using the STQN method.[16,17] The structural parameters of the transition state are given in Table 6. In the MP2 optimized structure, the H-atom has a distance of 120.7 pm from N_1 and 127.7 pm from N_2. The N_1N_2 distance in the transition state structure increases considerably from 136.1 pm for the 1*H*-tautomer and 133.4 pm for 2*H*-benzotriazole to 148.3 pm for the transition state geometry, while the N_2N_3 distance remains virtually constant. In contrast to 1*H*- and 2*H*-benzotriazole the H-atom is located out of plane for the transition state geometry, indicated by a dihedral angle $N_3N_2N_1H_1$ of 116.6° (A planar geometry of the TS, with an dihedral angle of 180° could be shown to be a *second*-order saddle point).

The (electronic) activation energy (2*H*-benzotriazole-transition state) amounts to 213 kJ mol^{-1} at the MP2 level, considering ZPE corrections it is calculated to be 195 kJ mol^{-1}. The two tautomers have an energy difference (including ZPE) of 7.75 kJ mol^{-1} with 2*H*-benzotriazole being the more stable tautomer. We have recently shown, that the determination of the correct energy order for this pair of tautomers requires at least forth order perturbation theory or CCSD with the 6-

Table 5 Experimental IR frequencies in cm^{-1} of benzotriazole$(H_2O)_2$ in the region of the –NH and –OH stretching vibrations together with calculated vibrational frequencies for different cluster structures. All calculations are performed at the MP2/6-31G(d,p) level of theory and are scaled by 0.95

		1*H*-BT$(H_2O)_2$		2*H*-BT$(H_2O)_2$
Assignment[a]	Experiment	a[b]	g	b
See text	3376	3097	3294	3094
OH (bound) 1	3389	3392	3571	3422
OH (bound) 2	3431	3487	3681	3493
OH (free) 1	3716.8	3759	3774	3762
OH (free) 2	3722.9	3763	3805	3767

[a] The assignment refers to the vibrational motion of the cyclic clusters. [b] This designation refers to Fig. 8 and Table 4.

Table 6 Bond lengths (Å), angles and dihedral angles (degrees) for three stationary points at the benzotriazole MP2/6-31G(d,p) potential energy surface. For atom numbering see Fig. 8

	1*H*-Benzotriazole	2*H*-Benzotriazole	Transition state
N_1H_1	1.008	2.037	1.277
N_2H_1	2.044	1.011	1.207
N_1N_2	1.361	1.334	1.483
N_2N_3	1.321	1.334	1.329
$N_1N_2N_3$	108.05	120.04	111.29
$N_2N_1H_1$	118.49	25.46	51.15
$N_3N_2N_1H_1$	180.00	180.00	116.50

311G(d,p) basis set.[1] The objective of this publication is to estimate the energy difference between the minima at the benzotriazole PES and the transition state connecting them. Due to the large activation energy, compared to the energy difference, the small errors due to insufficient basis set and method can be neglected. Fig. 9 shows the structures at the three stationary points of the benzotriazole PES (1*H*-benzotriazole, 2*H*-benzotriazole and TS).

2. Benzotriazole$(H_2O)_1$. The tautomerization between the binary water clusters of 1*H*- and 2*H*-benzotriazole is supposed to have a lower barrier than the reaction of the monomers, because the proton can be passed on through bond reorganizations in the water molecule, or for larger clusters in the water chain. The transition state for the tautomerization reaction between 1*H*-benzotriazole$(H_2O)_2$ and 2*H*-benzotriazole$(H_2O)_2$ has been calculated at the MP2/6-31G(d,p) level of theory using the STQN method.[16,17] Fig. 9 shows the geometry of the transition state for the interconversion of the two tautomeric clusters. The structural parameters of the transition state are given in Table 7. The water moiety, bridging the two tautomeric positions in the benzotriazole almost lies in the aromatic plane. The two H-atoms, connected to N_1 and N_2 have a considerably longer bond length than in a free water molecule. Intramolecular geometry parameters in the benzotriazole moiety are clearly less influenced than in the monomer TS. Especially, the distance between N_1 and N_2 remains nearly the same in the transition state structure, compared to the tautomers, while in the benzotriazole monomer a considerable increase in this bond length can be observed. The electronic energy difference calculated between the minimum energy structure of the cyclic 2*H*-benzotriazole$(H_2O)_1$ cluster and the transition state structure is calculated to be 137 kJ mol^{-1}, considering ZPE corrections 122 kJ mol^{-1}, while for the difference between the linear 2*H*-benzotriazole$(H_2O)_1$ cluster and the TS 138 kJ mol^{-1} (125 kJ mol^{-1} with ZPE) is calculated. The energy difference between the cyclic 1*H*- and 2*H*-benzotriazole$(H_2O)_1$ cluster is calculated to be 5.02 and 6.19 kJ mol^{-1} for the linear clusters (including ZPE and BSSE corrections). In both cases the 2*H*-tautomer is calculated to be the more stable one, of course with the same qualifications as made in the case of the monomer concerning basis set and method.

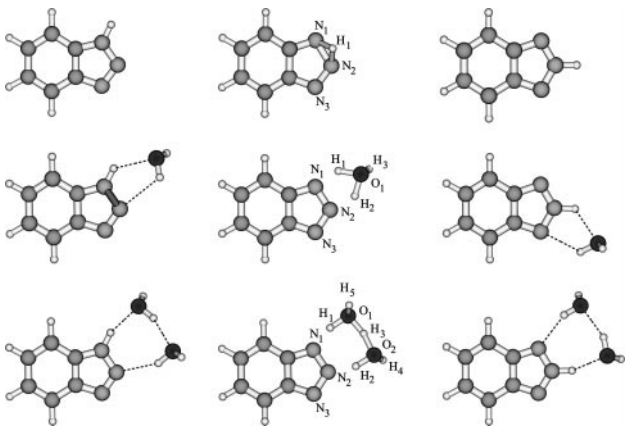

Fig. 9 Structures of 1*H*- and 2*H*-benzotriazole$(H_2O)_{0,1,2}$ and the respective transition state, connecting the tautomers as calculated at the MP2/6-31G(d,p) level of theory.

3. Benzotriazole$(H_2O)_2$. The tautomerization equilibrium between the 1 : 2 water clusters of 1*H*- and 2*H*-benzotriazole is supposed to have an even lower barrier, than the tautomerization between the monomers or the binary cluster, because the proton can be passed on through the water chain. The transition state for the tautomerization reaction between 1*H*-benzotriazole$(H_2O)_2$ and 2*H*-benzotriazole$(H_2O)_2$ has been calculated at the MP2/631G(d,p) level of theory using the STQN method.[16,17] The structural parameters of the transition state are given in Table 8, the resulting geometry is

Table 7 Bond lengths (Å), angles and dihedral angles (degrees) for three stationary points at the benzotriazole$(H_2O)_1$ MP2/6-31G(d,p) potential energy surface

	1*H*-Benzotriazole$(H_2O)_1$	2*H*-Benzotriazole$(H_2O)_1$	Transition state
N_1H_1	1.017	2.211	1.403
N_2H_2	2.226	1.019	1.421
N_1N_2	1.328	1.335	1.322
N_2N_3	1.255	1.331	1.274
O_1H_1	2.015	0.969	1.134
O_1H_2	0.969	2.045	1.126
O_1H_3	0.963	0.963	0.967
$N_1N_2N_3$	110.27	119.42	114.40
$N_1O_1N_2$	27.68	27.21	33.49
$N_3N_2N_1H_1$	178.85	179.43	178.37
$N_3N_2N_1H_2$	173.75	179.43	178.16
$N_3N_2N_1O_1$	176.73	176.94	177.86

Table 8 Bond lengths (Å), angles and dihedral angles (degrees) for three stationary points at the benzotriazole$(H_2O)_2$ MP2/6-31G(d,p) potential energy surface

	1*H*-Benzotriazole$(H_2O)_2$	2*H*-Benzotriazole$(H_2O)_2$	Transition state
N_1H_1	1.034	1.953	1.424
N_2H_2	1.952	1.036	1.446
N_1N_2	1.354	1.340	1.355
N_2N_3	1.327	1.331	1.336
O_1H_1	1.764	0.977	1.103
O_1H_4	0.963	0.962	0.966
O_1H_3	0.982	1.820	1.200
O_1O_2	2.739	2.756	2.393
O_2H_2	0.977	1.756	1.092
O_2H_3	1.791	0.980	1.216
O_2H_5	0.963	0.962	0.965
$N_1N_2N_3$	109.49	118.54	113.58
$N_2N_1O_1$	105.62	102.44	100.83
$N_1O_1O_2$	77.11	74.00	78.80
$O_1O_2N_2$	74.38	76.77	77.17
$N_3N_2N_1H_1$	179.86	178.52	179.40
$N_3N_2N_1H_2$	178.74	179.62	178.84
$N_3N_2N_1O_1$	179.13	178.86	179.30
$N_3N_2N_1H_3$	177.19	179.42	178.76
$N_3N_2N_1O_2$	176.71	179.16	178.61

shown in Fig. 9. For the transition state structure, both oxygen atoms of the water moieties, which bridge the N_1 and N_2-atom of benzotriazole are in the plane of the aromate. The three hydrogen atoms H_1, H_2 and H_3 are also positioned in this plane.

The energy difference calculated between the minimum energy structure of the cyclic 2*H*-benzotriazole$(H_2O)_2$ cluster and the transition state structure amounts to 101 kJ mol^{-1} (82 kJ mol^{-1} with ZPE), with an energy difference of 1.9 kJ mol^{-1} between the two tautomeric forms of the cluster (including ZPE and BSSE corrections), the 2*H*-tautomer being the more stable one.

The Gibbs energies of activation for the tautomeric equilibria of the monomers, 1 : 1 and 1 : 2 cluster, respectively have been calculated and are given in Table 9. From these Gibbs activation energies one can estimate the rate constants for the tautomerization using the relation:

$$k(T) = \frac{kT}{hc^{\ominus}} \exp\left(-\frac{\Delta G^{\neq}}{RT}\right) \quad (1)$$

Thus the relative tautomerization rate constants with the standard concentration $c^{\ominus}$ set to 1 can be estimated as 2×10^{-3} s^{-1} : 2×10^{-10} s^{-1} : 2×10^{-22} s^{-1} for the 1 : 2 cluster, the 1 : 1 cluster (cyclic and linear) and the monomer, respectively.

V. Discussion

The observation of three distinct electronic origins in the R2PI spectrum of the partially deuterated 1 : 1 cluster, and the IR–UV double resonance spectra in the region of the –OH and –NH stretching vibrations proved the 2*H*-benzotriazole$(H_2O)_1$ cluster to be cyclic. Two open questions remain. The first is concerned about the free –OH vibration in the electronic ground state of the cluster, which is obviously split into two sub-bands. The second question deals with the strange behavior of the vibronic spectrum, in which two band systems with nearly the same frequencies and intensities arise, separated by only 71 cm^{-1}. Geometry optimizations at the CIS level with the 6-311G(d,p) basis set predict a geometry of the benzotriazole monomer in the S_1 state in which the N–H group is slightly out-of-plane, which is in accordance with the slightly larger inertial defect in the electronically excited state, as obtained by Berden *et al.* using high resolution LIF spectroscopy.[5] The position of the H-atom above or below the aromatic plane leads to indistinguishable structures which are converted into each other *via* the inversion vibration at the central nitrogen atom. They represent *enantiomers* (the molecular symmetry group to describe their interconversion is the group G_4, consisting of the operations *E*, *P*, *E** and *P**), and have the same energy. For the benzotriazole–water cluster in the electronic ground state, the free H-atom of the water moiety points out of the plane, defined by the aromatic system. The positions above or below the plane have the same energy and the two orientations can also be interconverted by an inversion (group G_2, consisting of the operations *E*, and *E**). However, in the electronically excited state two *diastereomers* exist. In one of them, the hydrogen atom of benzotriazole and of the water moiety both point upwards (uu). In the other structure one points upwards and the other downwards (ud). The appearance of two band systems in the excitation spectrum could thus be explained by transitions to two different S_1 states which differ only slightly in their geometry. This leads to very similar vibrational frequencies and intensities of both band systems. The latter can be explained by the very small geometry change, which leads to similar Franck–Condon factors for both transitions. Based on these arguments and on a comparison of an *ab initio* mode analysis at

Table 9 Enthalpies and Gibbs energies of activation, reaction energies, enthalpies and Gibbs energies in kJ mol^{-1} for the tautomerization of benzotriazole and the benzotriazole–water clusters at the MP2/6-31G(d,p) level of theory

	$\Delta H^{\neq}$	$\Delta G^{\neq}$	ΔE^{298}	ΔH^{298}	ΔG^{298}
1*H*-BT $\rightleftharpoons$ 2*H*-BT	−195.10	−194.91	7.75	8.29	7.36
1*H*-BT$(H_2O)_1 \rightleftharpoons$ 2*H*-BT$(H_2O)_1$ (cyclic)	−117.91	−127.49	5.02	5.41	4.69
1*H*-BT$(H_2O)_1 \rightleftharpoons$ 2*H*-BT$(H_2O)_1$ (linear)	−124.18	−127.83	6.19	11.29	−8.68
1*H*-BT$(H_2O)_2 \rightleftharpoons$ 2*H*-BT$(H_2O)_2$	−76.69	−88.34	1.90	1.94	2.08

the CIS/6-31G(d,p) level, we performed an assignment of the vibronic bands of 2*H*-benzotriazole$(H_2O)_1$ which is given in Table 10. The vibronic transition at 26 cm^{-1} is assigned to a butterfly motion of the benzotriazole plane with respect to the plane of the water ring (ν_1). The ν_2 vibration at 61 cm^{-1} can be described as a cogwheel motion of these two rings relative to each other. At 103 cm^{-1} the stretching motion of the water moiety can be found (σ_1). The transition at 129 cm^{-1} is assigned to the combination band $\sigma + \nu_1$ and at 153 cm^{-1} to $\sigma + 2\nu_1$. The other vibronic transitions cannot be described unequivocally, because they represent superpositions with internal motions, located in the benzotriazole moiety.

The inversion motion of the free –OH in the binary cluster might also be responsible for the splitting observed in the –OH stretching vibration in the electronic ground state. In order to explain why this splitting does not show up as distinguishable bands in the double resonance experiments we have to postulate that the barrier to this inversion is of comparable height to the energy of the free –OH stretching vibration. Excitation of this vibration, which additionally might couple strongly to the inversion motion, results in a tunneling splitting, which is observed in the IR–UV double resonance spectrum. This splitting is not observable in the R2PI and UV–UV double resonance spectrum which can be attributed to the fact, that the analyzed transitions (all in the region of the electronic origin) connect levels in the ground and excited states which are well below the barrier and therefore virtually show no splitting.

The 2*H*-benzotriazole$(H_2O)_2$ cluster could be shown to be cyclic using IR–UV double resonance spectroscopy. As in the R2PI spectrum of the benzotriazole$(H_2O)_1$ cluster two band systems are observed, separated by 23 cm^{-1}. These are the electronic transitions into a pair of diastereomers from one ground state. Based on the cyclic structure we performed an *ab initio* normal mode analysis. The frequencies of the vibronic transitions in the region of the intermolecular vibrations are given in Table 11 and are compared with the frequencies of an *ab initio* normal mode analysis at the CIS//6-31G(d,p) level of theory. The vibronic transition at 11 cm^{-1} is assigned to an intermolecular vibration, which can be described as a linear combination of a twisting mode of the benzotriazole moiety *vs.* the water ring and a butterfly motion of the two respective ring systems (ν_1). The displacement vectors of this vibration are larger at the donor water moiety, while in the case of the ν_2 vibration at 34 cm^{-1}, which has a very similar motion, the displacements are larger at the acceptor water moiety. The third fundamental at 67 cm^{-1} can be described as a cogwheel motion of the water ring *vs.* the benzotriazole moiety. Its motion and frequency is very similar to the corresponding vibration in the cyclic phenol–water clusters.[23] The range of these mutual ring motions is followed by a region of little vibronic activity. The intermolecular stretching vibrations start at 133 cm^{-1}, with the stretching of the donor water (σ_1), followed by the acceptor water stretching vibration at 153 cm^{-1} (σ_2). The next three vibrations (ν_4–ν_6) can be attributed to water ring deformation vibrations.

VI. Conclusions

From the comparison of the UV and IR–UV spectra of the benzotriazole water clusters and their deuterated isotopomers with the results of *ab initio* normal mode analysis, we could show that the 1 : 1 and the 1 : 2 clusters have cyclic structures in the electronic ground and excited state, with one and two water moieties bridging the >N̄H and =N̄– functional groups

Table 10 Experimental intermolecular vibrations of the two band systems of 2*H*-benzotriazole$(H_2O)_1$ together with the CIS/6-31G(d,p) vibrational frequencies for the cyclic 2*H*-benzotriazole$(H_2O)_1$ cluster. All frequencies are given in cm^{-1}

		Experiment		
Assignment	Description	Band system 1	Band system 2[a]	2*H*-BT$(H_2O)_1$ CIS/6-31G(d,p)
0,0		0	0	0
ν_1	Butterfly	26	24	34.8
ν_2	Cogwheel	61	61	57.2
σ	Stretch	103	100	135.2
$\sigma + \nu_1$		129	—	—
ν_3		146	146	157.6
$\sigma + 2\nu_1$		153	—	—
$\nu_2 + \sigma$		164	168	—
ν_4		184	184	212.3
ν_5		190	193	218.2

[a] All frequencies relative to the origin of B.S. 2 at 71 cm^{-1}.

Table 11 Experimental intermolecular vibrations of 2*H*-benzotriazole$(H_2O)_2$ together with the CIS/6-31G(d,p) vibrational frequencies for the cyclic 2*H*-benzotriazole$(H_2O)_2$ cluster. All frequencies are given in cm^{-1}

		Experiment		
Assignment	Description	Band system 1	Band system 2[a]	2*H*-BT$(H_2O)_2$ CIS/6-31G(d,p)
0,0		0	0	0
ν_1	Twist + butterfly	11	11	31.8
ν_2		45	44	36.3
ν_3	Cogwheel	56	55	61.3
σ_1	Stretch BT acceptor	133	133	138.3
σ_2	Stretch BT donor	153	152	149.6
ν_4		183	183	179.4
ν_5	Water ring deformations	196	195	198.2
ν_6		212	213	213.4

[a] All frequencies relative to the origin of B.S. 2 at 23 cm^{-1}.

of the chromophore. For the benzotriazole$(H_2O)_2$ cluster, this cyclic structure was calculated at the MP2/6-31G(d,p) level to be the lowest energy structure, while for the 1 : 1 cluster the linear donor structure was found to be energetically slightly favored over the cyclic structure. Nevertheless this structure was found to be a first-order saddle point at the PES instead of a true minimum. Based on the minimum energy structures which have been derived from the double resonance experiment we performed a normal mode analysis at the fully optimized CIS geometry of the clusters. The results are in agreement with the experimental findings, although there are considerable numerical deviations due to the insufficient theoretical method applied.

The cyclic geometries anticipate the structure of the transition state for the tautomerization of 1*H*- to 2*H*-benzotriazole in the cluster. *Ab initio* calculations show that the energy difference between the two tautomers and the activation energy for the tautomerization decrease with increasing cluster size. This decrease in activation energy can be attributed to a mechanism of passing the hydrogen atom "through" the chain of water molecules, similar as in the Grotthus mechanism of proton conductivity in liquid water. The great increase in tautomerization rate upon going from the monomer to the $n = 2$ cluster suggests the possibility of a proton transfer in the electronic ground state even for small cluster sizes.

Acknowledgements

We thank the Deutsche Forschungsgemeinschaft for financial support of this work (SCHM1043/9-1). Helpful discussions with Ch. Jacoby are gratefully acknowledged. This work is part of the Ph.D. thesis of Ch. Plützer.

References

1 W. Roth, D. Spangenberg, C. Janzen, A. Westphal and M. Schmitt, *Chem. Phys*., 1999, **248**, 17.
2 B. Velino, E. Canè, L. Gagliardi, A. Trombetti and W. Caminati, *J. Mol. Spectrosc*., 1993, **161**, 136.
3 F. Negri and W. Caminati, *Chem. Phys. Lett*., 1996, **260**, 119.
4 E. Jalviste and A. Treshchalov, *Chem. Phys*., 1993, **172**, 325.
5 G. Berden, E. Jalviste and M. L. Meerts, *Chem. Phys. Lett*., 1994, **226**, 305.
6 W. Roth, C. Jacoby, A. Westphal and M. Schmitt, *J. Phys. Chem*., A, 1998, **102**, 3048.
7 G. Fischer, X. Cao and R. L. Purchase, *Chem. Phys. Lett*., 1996, **262**, 689.
8 A. Bigotto, A. N. Pandey and C. Zerbo, *Spectrosc. Lett*., 1996, **29**, 511.
9 J. Catalán, P. Pérez and J. Elguero, *J. Org. Chem*., 1993, **58**, 5276.
10 F. Tomás, J. Catalán, P. Pérez and J. Elguero, *J. Org. Chem*., 1994, **59**, 2799.
11 C. Jacoby, W. Roth and M. Schmitt, *Appl. Phys. B*, 2000, **71**, 643.
12 M. Schmitt, C. Jacoby and K. Kleinermanns, *J. Chem. Phys*., 1998, **108**, 4486.
13 A. R. H. Cole, *Tables of Wavenumbers for the Calibration of Infrared Spectrometers*, Pergamon Press, Oxford, 2nd edn., 1977.
14 M. J. Frisch, G. W. Trucks, H. B. Schlegel, G. E. Scuseria, M. A. Robb, J. R. Cheeseman, V. G. Zakrzewski, J. A. Montgomery, Jr., R. E. Stratmann, J. C. Burant, S. Dapprich, J. M. Millam, A. D. Daniels, K. N. Kudin, M. C. Strain, O. Farkas, J. Tomasi, V. Barone, M. Cossi, R. Cammi, B. Mennucci, C. Pomelli, C. Adamo, S. Clifford, J. Ochterski, G. A. Petersson, P. Y. Ayala, Q. Cui, K. Morokuma, D. K. Malick, A. D. Rabuck, K. Raghavachari, J. B. Foresman, J. Cioslowski, J. V. Ortiz, A. G. Baboul, B. B. Stefanov, G. Liu, A. Liashenko, P. Piskorz, I. Komaromi, R. Gomperts, R. L. Martin, D. J. Fox, T. Keith, M. A. Al-Laham, C. Y. Peng, A. Nanayakkara, C. Gonzalez, M. Challacombe, P. M. W. Gill, B. Johnson, W. Chen, M. W. Wong, J. L. Andres, C. Gonzalez, M. Head-Gordon, E. S. Replogle and J. A. Pople, *GAUSSIAN 98*, *Revision A.7*., Gaussian Inc., Pittsburgh, PA, 1998.
15 S. F. Boys and F. Bernardi, *Mol. Phys*., 1970, **19**, 553.
16 C. Peng, P. Y. Ayala, H. B. Schlegel and M. J. Frisch, *J. Comput. Chem*., 1996, **17**, 49.
17 C. Peng and H. B. Schlegel, *Israel J. Chem*., 1994, **33**, 449.
18 J. R. Carney, F. C. Hagemeister and T. S. Zwier, *J. Chem. Phys*., 1998, **108**, 3379.
19 J. R. Carney and T. S. Zwier, *J. Phys. Chem. A*, 1999, **103**, 9943.
20 H. Watanabe and S. Iwata, *J. Chem. Phys*., 1996, **105**, 420.
21 J. B. Paul, R. A. Provencal, C. Chapo, K. Roth, R. Casaes and R. J. Saykally, *J. Phys. Chem. A*, 1999, **103**, 2972.
22 T. Ebata, A. Fujii and N. Mikami, *Int. J. Mass Spectrom. Ion Processes*, 1996, **159**, 111.
23 C. Jacoby, W. Roth, M. Schmitt, C. Janzen, D. Spangenberg and K. Kleinermanns, *J. Phys. Chem. A*, 1998, **102**, 4471.